Iraq Salinity Project **Technical Report 1**

Development of Salinity Models by Remote Sensing in Central and Southern Iraq

Reporters

Weicheng Wu (ICARDA), Ahmad S. Mhaimeed (MoHE), Alexander Platonov (IWMI), Waleed M. Al-Shafie (MoA), Ayad H. Abbas (MoWR), Hassan H. Al-Musawi (MoWR), Abdu Jabbar Khalaf (MoWR), Feras Ziadat (ICARDA)

The Iraq Salinity Project is an initiative of Government of Iraq, Ministries of Agriculture, Water Resources, Higher Education, Environment, and Science and Technology, and an international research team led by ICARDA – the International Center for Agricultural Research in the Dry Areas, in partnership with the University of Western Australia, the Commonwealth Scientific and Industrial Research organization (CSIRO) of Australia, the International Water Management Institute (IWMI), Sri Lanka, and the International Center for Biosaline Agriculture (ICBA), Dubai, United Arab Emirates.

This research is funded by the Australian Centre for International Agricultural Research (ACIAR), AusAID and the Italian Government.

This technical report series captures and documents the work in progress of the Iraq Salinity Project, in its seven research themes, working at the regional, farm and irrigation system scales. Technical reports feed into the *Iraq Salinity Assessment*, a synthesis and solutions to solving the problem: Situation Analysis (Report 1); Approaches and Solutions (Report 2) and Investment Options (Report 3).

Key words: salinity models, central and southern Iraq, multi-temporal approach, vegetation, non-vegetation indices.

This report was written and compiled by:

Dr Weicheng Wu (ICARDA), Dr Ahmad S. Mhaimeed (MoHE), Dr Alexander Platonov (IWMI), Mr Waleed M. Al-Shafie (MoA), Dr Ayad H. Abbas (MoWR), Dr Hassan H. Al-Musawi (MoWR), Dr Abdu Jabbar Khalaf (MoWR), Dr Feras Ziadat (ICARDA)

http://icarda.org/iraq-salinity-project/teaser

1. Background

As defined in the project proposal, the main target of Component A (ACIAR Project) and Component 1 (Italian Project) is to quantify the spatial distribution of salt-affected land in the central and southern Iraq based on multi temporal and multi scale remote sensing approach. The critical part of this approach, in spite of challenging (see our mid-term report for detail), is the development of salinity models on which salinity intensity assessment in space and time, and mapping are based. This report is demonstrating the procedure of the development of salinity models in the pilot sites, and their integration for regional scale assessment and mapping. The developed models are not only applicable in Mesopotamia in Iraq but also valid for other dryland areas with same or similar environmental condition.

The model development can be divided into two levels: local/pilot site scale and regional scale.

2. Local scale: Pilot site study

Local scale studies are dealing with the development of salinity models in pilot sites in Mesopotamia. As proposed by stakeholders (Ministry of Agriculture, Ministry of Water Resources, Ministry of Environment and Ministry of Sciences and Technology of Iraq Government), five pilot sites were selected, of which four sites (Musaib, Dujaila, Abu Khseeb and Shat-Al-Arab) were identified in the frame of ACIAR Project and one (West Gharraf in Nassirieh) in the Italian Project. In terms of the data availability, we focused our salinity modelling work on three sites namely Musaib, Dujaila and West Gharraf.

2.1 Method

Having been fully aware of the difficulty and challenge to assess salinity by remote sensing just using one date image (see our mid-term report), we proposed a field sampling-based multiyear remote sensing method, that is, to utilize multiyear spring and summer data by taking into account land management and practice, e.g. crop rotation and fallow state. It is known that fallow state will generally last 2-3 years in Iraq; if we consider an observation period of four years, the problem related to fallow can be avoided given that salinity does not change significantly in such a time period.

2.1.1 Data

As mentioned, multiyear satellite imagery, especially, Landsat ETM+ images from February 2009 to August 2012 (see table 1) and field sampling and investigation data (table 2 for various sampling number, Output A1.2) were used for modelling.

2.1.2 Procedures

The procedure is unfurled as follows:

(1) Atmospheric correction of the Landsat ETM+ images using FLAASH model.

(2) Multispectral transformation of a set of vegetation and non-vegetation indices such as NDVI (Normalized Difference Vegetation Index, Rouse et al. 1973), EVI (Enhanced Vegetation Index, Huete et al. 1997), SAVI (Soil Adjusted Vegetation Index, Huete 1988), SARVI (Soil Adjusted and Atmospherically Resistant Vegetation Index, Kauffmann and Tanre 1992), NDII (Normalized Difference Infrared Index, Hardisky et al. 1983). We also introduced a new vegetation index namely GDVI (Generalized Difference Vegetation Index) developed by Wu (2012) and in form of

$$GDVI = \frac{\rho_{NIR}^{n} - \rho_{R}^{n}}{\rho_{NIR}^{n} + \rho_{R}^{n}}$$

where ρ_{NIR} and ρ_{R} are respectively reflectance of the near infrared (NIR) and red (R) bands, and *n* is power number, an integer of the values of 1, 2, 3, 4... *n*. The dynamic range of GDVI is the same as NDVI from -1 to 1; when *n* = 1, GDVI = NDVI. This index can largely amplify vegetation information for low vegetated areas such as dryland ecosystem and is better correlated with LAI (Leaf Area Index) than any other vegetation index. In this research, we used GDVI, of which power number *n* = 2, that is,

$$GDVI\text{^}2 = \frac{\rho_{NIR}^{2} - \rho_{R}^{2}}{\rho_{NIR}^{2} + \rho_{R}^{2}}$$

Table 1: Landsat ETM+ images used for salinity model development

Musaib			Dujaila and West Gharraf		
Frame: 168-37			Frame: 167-38		
Spring	**June**	**Summer**	**Spring**	**June**	**Summer**
2009-03-17	2009-06-05	2008-08-05	2009-03-26	2010-06-01	2009-09-02
2009-04-18	2010-06-08	2010-08-11	2009-04-11	2012-06-06	2010-08-20
2010-03-20	2011-06-11	2011-08-14	2010-03-29	2012-06-22	2011-08-23
2011-02-03	2012-06-13	2012-08-16	2011-04-17		2012-08-25
2011-02-19		2012-09-01	2012-04-03		
2012-02-22			2012-04-19		
2012-03-09					
2012-04-26					

Table 2: Field sampling and investigation (Output A1.2)

Sites	Soil Profile (0-100cm)	Surface Soil Samples (0-30cm)		EM38		AccuPAR Mar-Apr 2012
		Jul 2011-Apr 2012	Supplemental Jun-Jul 2012	Mar-Apr 2012	Supplemental Jun-Jul 2012	
Musaib	13	30	6	45	23	36
Dujaila	5	17	6	65	17	17
West Garraf(Italian)		22	4	57	17	15
Shat-Al-Arab	4	16		54		36
Abu Khaseeb	5			15		15
Transects						
Transect 1		20		60		60
Transect 2		44		132		25
Total	27	165		485		204

As for non-vegetation indices, they are Principal Components (especially the 1st and 2nd components denoted as PC1 and PC2), the maximum spring surface temperature (ST) from February to April, summer (August) temperature (AT) and Tasselled Cap Brightness (BRT, Crist et al. 1984 and Huang et al. 2002), derived from Landsat ETM+ imagery.

(3) Derivation of the multiyear maximum value in each pixel of each index in the observed period 2009-2012 to avoid problems related to crop rotation and fallow, and gaps left by the SLC-Off problem in ETM+ images.

(4) Extraction of the values of each vegetation and non-vegetation index corresponding to the field sampling locations (about 3 to 5 controversial samples very close to the roads or located in fallow land were excluded).

(5) Coupling remote sensing indicators with the available EM38 measurement and soil electrical conductivity (EC) data using multiple linear least-square regression analysis at the confidence level of 95% in a stepwise (forward) manner.

One point to be noted here is that the vertical and horizontal EM38 readings (denoted respectively as EMV and EMH) are the average value of three subplots (1m × 1m) distributed at the corners of a triangle with a distance of 15-20 m between each of two subplots, to match largely the pixel size of Landsat images (30 m).

The concrete steps for this modelling are shown below:

1) Arrange field data in Excel and make it importable for ArcGIS (including coordinators normalization, E/N or Lat/Long), averaging data in the same plot but different readings in three subplots
2) Add both remote sensing indicators in TIF format and Excel field data (Points) to ArcGIS
3) Use Spatial Analyst Tools to extract the values of remote sensing indicators corresponding to the field sampling plots
4) Conversion of the remote sensing indicators variables into exponential and logarithmic forms
5) Input separately VIs and non-vegetation indices into SYSTAT or GenSTAT
6) Using multiple linear least-square regression model to calibrate respectively the EMV/EMH or EC with VIs and NonVIs

2.2 Results

The results reveal that soil salinity and EM38 readings are negatively correlated with the different vegetation indices, especially, GDVI, NDVI, SAVI and EVI, and positively correlated with ST, PC1 and BRT. We have to mention that the correlation between remote sensing indicators and EM38 readings undertaken in March-April 2012 is low for both Musaib and West Gharraf; however, it is very high between the supplemental sampling readings and remote sensing indicators in all the three sites. The main reason is that the supplemental sampling was conducted in June and early July, when harvesting of spring crops such as wheat, barley was finished and large-scale summer irrigation was not yet started. Thus, the moisture influences on EM38 readings can be greatly minimized in this dry season. The models obtained for the pilot sites Musaib, Dujaila and West Gharraf are respectively presented as follows.

2.2.1 Salinity models

In the course of modelling, we undertook first the correlation analysis to understand which remote sensing indicator(s) is (are) mostly associated with soil salinity, followed with a least-square linear regression analysis to establish the relationships between salinity (EC or EMV/EMH, the dependent variable) and remote sensing indicators (independent variables). So both correlation coefficients multiple linear regression models are presented respectively in tables 3a, 3b, 4a, 4b, 5a and 5b, and table 6.

Table 3a: Correlation coefficients between EM38 readings and VIs in Musaib

	SAVI	Exp(SAVI)	Ln(SAVI)	GDVI	Ln(GDVI)	Exp(GDVI)	EVI	Exp(EVI)
EMV	-0.82	-0.787	-0.904	-0.901	-0.936	-0.875	-0.843	-0.808
EMH	-0.798	-0.767	-0.878	-0.875	-0.904	-0.852	-0.821	-0.789

	Ln (EVI)	ST	Exp(ST)	Ln(ST)	NDVI	Ln(NDVI)	Exp(NDVI)
EMV	-0.914	0.859	0.743	0.857	-0.843	-0.914	-0.808
EMH	-0.885	0.844	0.741	0.843	-0.821	-0.885	-0.789

Table 3b: Correlation coefficients between EM38 readings and NonVIs in Musaib

	PC1	Exp(PC1)	PC2	Exp(PC2)	PC3	Exp(PC3)	TC_BRT	Ln(BRT)	Exp(BRT)
EMV	0.749	0.757	-0.559	-0.55	0.548	0.55	0.586	0.572	0.59
EMH	0.737	0.747	-0.527	-0.519	0.614	0.617	0.576	0.56	0.581

	NDII45	Exp(NDII45)	Ln(NDII45)	ST	Exp(ST)	Ln(ST)
EMV	-0.692	-0.672	-0.723	0.859	0.764	0.858
EMH	-0.685	-0.664	-0.718	0.849	0.798	0.847

Table 4a: Correlation coefficients between VIs and EM 38 readings in the Dujaila site

	SAVI	SARVI	NDVI	GDVI	EVI	NDII45	Exp(GDVI)	Exp(NDVI)
EMV	-0.824	-0.82	-0.839	-0.854	-0.798	-0.783	-0.854	-0.822
EMH	-0.791	-0.781	-0.807	-0.832	-0.759	-0.743	-0.827	-0.786

	Exp(EVI)	Exp(SAVI)	Ln(EVI)	Ln(GDVI)	Ln(NDVI)	Ln(SAVI)
EMV	-0.741	-0.813	-0.819	-0.824	-0.838	-0.829
EMH	-0.697	-0.777	-0.79	-0.811	-0.819	-0.811

Table 4b: Correlation coefficients between NonVIs and EM 38 readings in the Dujaila site

	ST	Ln(ST)	PC1	Exp(PC1)	PC2	Exp(PC2)	BRT	Exp(BRT)	Ln(BRT)
EMV	0.728	0.727	0.638	0.639	0.565	0.564	0.594	0.592	0.595
EMH	0.714	0.713	0.591	0.591	0.556	0.556	0.592	0.539	0.546

Table 5a: Correlation coefficients between VIs and EM 38 readings in the West Gharraf site

	GDVI	Exp(GDVI)	Ln(GDVI)	EVI	Exp(EVI)	Ln(EVI)	NDII57	Exp(NDII57)	Ln(NDII57)
EMV	-0.806	-0.79	-0.827	-0.781	-0.752	-0.826	-0.599	-0.602	-0.562
EMH	-0.721	-0.706	-0.739	-0.698	-0.669	-0.744	-0.458	-0.464	-0.407

	NDVI	Exp(NDVI)	Ln(NDVI)	SARVI	Exp(SARVI)	SAVI	Exp(SAVI)	Ln(SAVI)
EMV	-0.794	-0.782	-0.825	-0.771	-0.763	-0.792	-0.784	-0.821
EMH	-0.709	-0.698	-0.737	-0.669	-0.663	-0.71	-0.702	-0.738

Table 5b: Correlation coefficients between Non-vegetation indices and EM 38 readings in the West Gharraf site

	ST	Exp(ST)	Ln(ST)	BRT	Exp(BRT)	Ln(BRT)	PC1	Exp(PC1)	PC2	Exp(PC2)
EMV	0.760	0.526	0.760	0.791	0.791	0.790	0.754	0.751	0.174	0.168
EMH	0.621	0.376	0.621	0.682	0.683	0.679	0.633	0.629	0.088	0.082

Table 6: Salinity models obtained in the pilot sites

Sites	Type	Equations	Error scope	Multiple R^2
Musaib	Vegetated area	EMV = -824.134 + 918.536*GDVI - 754.204*ln(GDVI) EMH = -606.197 – 460.043*ln(GDVI) + 245.086*Exp(GDVI)	± 41.700 ± 48.559	0.925 0.862
	Non-Vegetated area	EMV = 2570683.24 + 1821.24ST – 546476.07*ln(ST) EMH = 2608853.46 + 1842.4ST– 554286.69*ln(ST)	± 62.944 ± 51.217	0.829 0.846
Dujaila	Vegetated area	EC = -21.584*ln(GDVI) – 2.630 (dS/m) EMV = 2606.137 + 672.195*SARVI – 2761.563*GDVI + 750.73*ln(NDVI)	± 6.273 ± 58.543	0.809 0.783
	Non-Vegetated area	EMV= 2119573.641 + 1507.489*ST – 450880.891*ln(ST) EMH = 2118582.448 + 1499.761*ST – 450307.069*ln(ST)	± 60.813 ± 79.024	0.582 0.610
West Gharraf	Vegetated area	EMV = 579.604 – 708.696*ln(GDVI) + 611.04*ln(NDII57)	± 102.155	0.852
	Non-Vegetated area	EMV=-1294.669 + 2611.279*BRT	± 156.603	0.626

It is clear from the above tables that remote sensing salinity model in different pilot sites is slightly different due to the difference in background (soil, irrigation and cultivation…). For vegetated areas, GDVI is the best salinity indicator, followed by SARVI, NDVI and NDII, whereas in the non-vegetated areas the spring maximum temperature (ST) is the best indicator followed by the Tasseled Cap Brightness (BRT) although the multiple R^2 in Dujaila and West Gharraf is not very high (0.582– 0.626). This can be improved with more field samples taken in bareland (including bare soil, saline soil and desert) in future.

Using RapidEye and SPOT imagery, rather strong correlation between EM38 readings and remote sensing vegetation indices such as GDVI, NDVI and SAVI was also obtained (R^2 = 0.671-0.769). The shortcoming is that there was no thermal band in these images and thus no possibility to derive surface temperature. Another disadvantage is that it is almost impossible to get more than one acquisition for the same site in 3-4 year period, and hence the problem derived from crop rotation and fallow cannot be avoided.

2.2.2 Relationships between EMV/EMH and EC

Based on the lab analytical results of the regional samples along transects and in pilot sites, the relationships between EMV/EMH and soil salinity, e.g. electrical conductivity (EC) was obtained (Figure 1). These relationships allow us to convert EMV and EMH equations into EC models (dS/m).

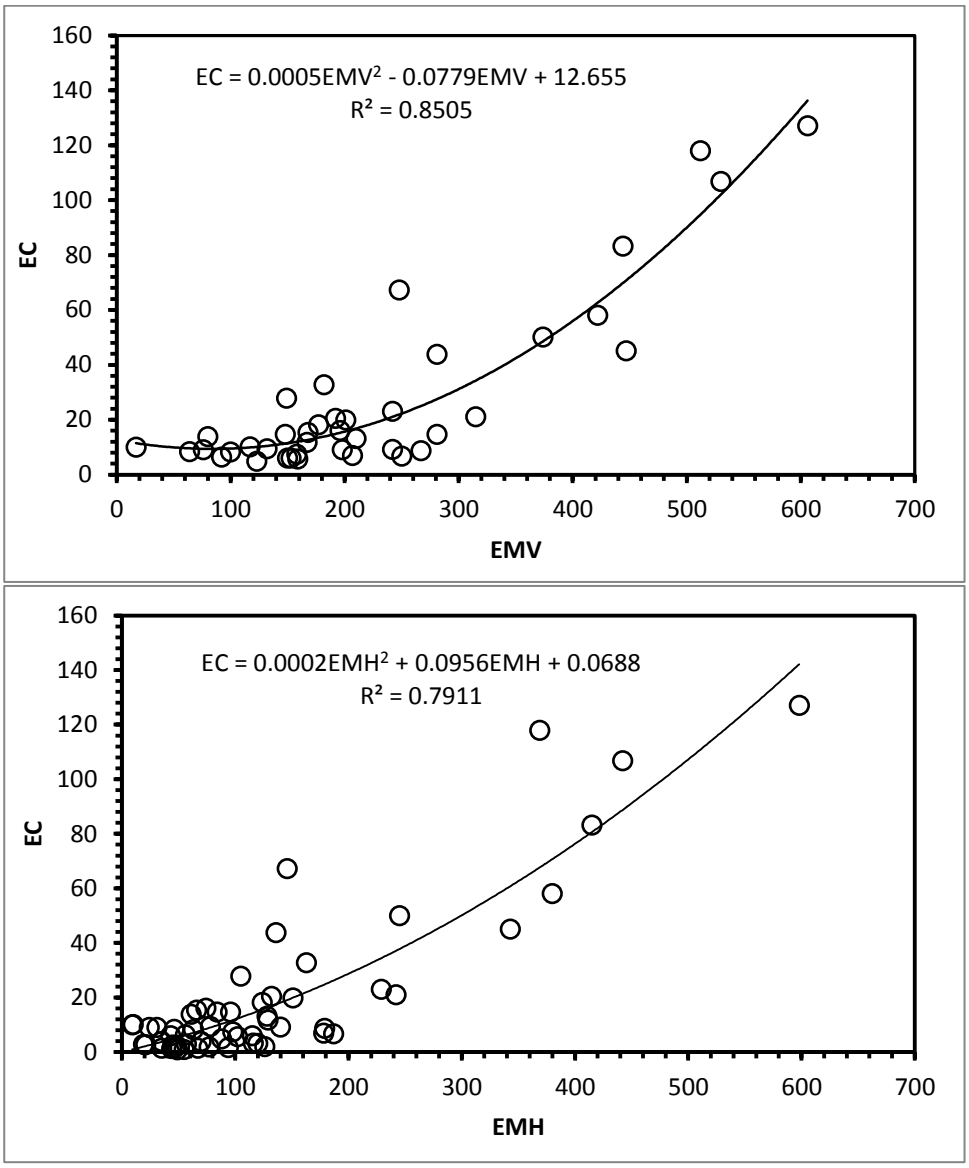

Figure 1: Relationships between EC and EMV/EMH

2.2.3 Validation of models

After obtaining the salinity models, one key issue is to check their validity, more concretely, to investigate whether these models are operational.

For this purpose, we applied respectively the models of Musaib to the VIs and NonVIs of Musaib and the models of Dujaila to the remote sensing indicators of Dujaila to produce salinity maps (detail will be unfurled in our Output A1.4: Multitemporal salinity mapping). The accuracy of the salinity maps against the ground measurement in Musaib and Dujaila is respectively 81.1% and 80.7%. This means that remote sensing estimated salinity is reliable and the models are operational.

3. Regional scale salinity models

As we have already noted, in different pilot sites salinity models are not the same, and none of them can be directly applied for regional salinity analysis due to the difference in locality (e.g. soil, irrigation, dominant cultivation). For regional scale assessment, we have to take account of such difference in background and

spatial representativeness of sampling. Hence, it is necessary to combine the data from the three pilot sites together to derive regionally applicable models.

After integration of the data from the three sites, multiple linear regression analyses were applied again to the stacked data and very promising results were obtained. The correlation coefficients are shown in table 7a and 7b, and regional salinity models in equations (1) and (2):

Table 7a: Regional scale correlation coefficients between EM38 readings and VIs

	SAVI	Exp(SAVI)	Ln(SAVI)	GDVI	Ln(GDVI)	Exp(GDVI)	EVI	Exp(EVI)
EMV	-0.768	-0.745	-0.833	-0.818	-0.847	-0.795	-0.664	-0.584
EMH	-0.691	-0.666	-0.771	-0.746	-0.789	-0.718	-0.598	-0.516

	Ln(EVI)	NDVI	Exp(NDVI)	Ln(NDVI)
EMV	-0.772	-0.777	-0.748	-0.840
EMH	-0.717	-0.698	-0.667	-0.775

Table 7b: Regional scale correlation coefficients between EM38 readings and NonVIs

	PC1	Exp(PC1)	PC2	Exp(PC2)	BRT	Ln(BRT)	Exp(BRT)	ST	Exp(ST)	Ln(ST)
EMV	0.614	0.613	0.093	0.078	0.670	0.658	0.675	0.757	0.555	0.755
EMH	0.540	0.539	0.079	0.066	0.586	0.575	0.59	0.677	0.509	0.675

For vegetated areas:

$EMV = 66.338 - 258.114 * \ln(GDVI) \pm 88.882$ (multiple $R^2 = 0.717$) (1)

Non-Vegetated areas:

$EMV = 2874415.66 + 2035.443 * ST - 610991.724 * \ln(ST) \pm 97.653$ (multiple $R^2 = 0.662$) (2)

In spite of the lower correlation coefficients in comparison with the models at local scale, the GDVI and ST are always the best salinity indicators respectively for vegetated and non-vegetated areas at regional scale. These models shed light on the possibility of regional salinity assessment. However, whether these models — equations (1) and (2), are applicable and operational for regional salinity mapping will be discussed in Output A2.2: Regional salinity mapping.

4. Summery

In spite of challenge, remote sensing-based salinity models were developed for both pilot site and regional scale salinity mapping and assessment. Due to the quality problem of Landsat ETM+ imagery, these models are not perfect and can be improved when more new images, especially, Landsat 8 images and more field samples taken in bareland are available.

References:

Hardisky, M. A., Klemas, V. and Smart, R. M. (1983). The influences of soil salinity, growth form, and leaf moisture on the spectral reflectance of *Spartina alterniflora* canopies. Photogrammetric Engineering & Remote Sensing, 49, 77-83.

Huete, A. R., (1988). A soil adjusted vegetation index (SAVI). Remote Sensing of Environment, 25, 295–309.

Huete, A. R., Liu, H. Q., Batchily, K., and van Leeuwen, W. (1997). A comparison of vegetation indices global set of TM images for EOS-MODIS. Remote Sensing of Environment, 59, 440-451

Kaufman, Y. J. and Tanré, D. (1992). Atmospherically resistant vegetation index (ARVI) for EOS-MODIS. *IEEE Transactions on Geoscience and Remote Sensing,* **30**, pp.261-270.

Rouse, J. W., Haas, R. H., Schell, J. A. and Deering, D. W. (1973). Monitoring vegetation systems in the Great plains with ERTS. In: Proceedings of the Third ERTS-1 Symposium, NASA SP-351, 1, 309-317.

Wu, W. (2012). The Generalized Difference Vegetation Index (GDVI) for land characterization. Presented in 8th ISSC (International Soil Science Congress, Izmir, Turkey, May 15-17, 2012) and selected for publication in Journal "Soil & Tillage Research (STILL)".